Production of Oxymethylene Dimethyl Ethers from Hydrogen and Carbon Dioxide - Part II: Modeling and Analysis for OME_{3-5}

Journal:	*Industrial & Engineering Chemistry Research*
Manuscript ID	ie-2018-05577k.R2
Manuscript Type:	Article
Date Submitted by the Author:	13-Mar-2019
Complete List of Authors:	Burre, Jannik; Rheinisch Westfalische Technische Hochschule Aachen, Process Systems Engineering (AVT.SVT) Bongartz, Dominik; Rheinisch Westfalische Technische Hochschule Aachen, AVT.SVT Mitsos, Alexander; Rheinisch Westfalische Technische Hochschule Aachen, AVT.SVT

Production of Oxymethylene Dimethyl Ethers from Hydrogen and Carbon Dioxide – Part II: Modeling and Analysis for $OME_{3\text{-}5}$

Jannik Burre,[†] Dominik Bongartz,[†] and Alexander Mitsos[*,‡,†,¶]

[†]*Process Systems Engineering (AVT.SVT), RWTH Aachen University, Forckenbeckstr. 51, 52074 Aachen, Germany*

[‡]*JARA-ENERGY, 52056 Aachen, Germany*

[¶]*Energy Systems Engineering (IEK-10), Forschungszentrum Jülich, 52425 Jülich, Germany*

E-mail: amitsos@alum.mit.edu

Phone: +49 241 80 94808. Fax: +49 241 80 92326

Abstract

Oxymethylene dimethyl ethers (OME_n) have a high potential as diesel fuels or blending components due to their promising combustion properties and can be produced from hydrogen (H_2) and carbon dioxide (CO_2) by combining existing process concepts. However, such a process chain has not been analyzed in detail yet, so that its performance and bottlenecks are unknown. In this second part of our two-part article, we analyze a process chain for production of the longer chain variant $OME_{3\text{-}5}$ from renewable H_2 and green CO_2 via trioxane and OME_1. We simulate in Aspen Plus® using detailed thermodynamic models with coupled oligomerization reactions and rigorous unit operation models. The overall exergy efficiency of $OME_{3\text{-}5}$ production from H_2 and CO_2 using established process concepts is 53%. Therein, the trioxane process

step has the highest losses due to its high heat demand. Considering a pinch-based heat integration throughout the entire process chain its total heat demand can be reduced by 16%. Thus, the exergy efficiency increases to 54%. This is still significantly lower compared to the production of other alternative fuels like OME_1, methane, and dimethyl ether. Thus, more efficient processes, e.g., by avoiding trioxane production, are required.

1 Introduction

One option for climate change mitigation is the conversion of renewable electricity to combustion engine fuels with a suitable carbon source. Bongartz et al.[1] assess four alternative transportation fuels from renewable energy addressing various performance and handling aspects, e.g., infrastructure compatibility and environmental impacts. Dimethyl ether (DME) is found to be promising in terms of emissions, whereas its infrastructure compatibility is rather low. For the direct use of hydrogen (H_2) in fuel cell vehicles (FCV) this factor is even more serious, as required infrastructure changes are expected to be particularly expensive because of the high pressure required for effective storage, distribution, and fueling.[1] In contrast, hydrocarbons produced from Fischer-Tropsch (FT) synthesis are compatible with today's infrastructure, but do not offer benefits regarding pollutant emissions.[2]

An alternative fuel that does have such benefits is the group of oxymethylene dimethyl ethers (OME_n, $CH_3O(CH_2O)_nCH_3$). Part one of this two-part article analyzed the production of OME_1 from renewable H_2 and green carbon dioxide (CO_2) with existing technology and demonstrated the potential for efficiency improvements and process simplifications based on process modifications. However, missing compatibility of OME_1 and OME_1-diesel blends with conventional combustion engines are reported by many publications[3–5] and are disadvantages for market penetration. In contrast, OME_n with three to five FA groups (hereafter referred to as $OME_{3\text{-}5}$) have very similar fuel properties to diesel and, thus, do not require major modifications to the injection system.[2–4,6] Their potential of having a lower

global warming impact (GWI) compared to conventional diesel and the avoided soot-NO_x trade-off[7] give them promising properties as a potential diesel blend or even as a complete replacement of conventional diesel.[8] Additionally, $OME_{3\text{-}5}$ blends may even increase engine efficiency[2] and, thus, improve fuel economy.[9] Nowadays, $OME_{3\text{-}5}$ are produced industrially in China at a scale of more than 240,000 t/a.[10] Since their production is based on coal and future mobility is supposed to be environmentally friendly, novel production processes need to be based on a renewable feedstock.

Due to increasing interest in OME_n as a synthetic fuel, much effort is being spent on new synthesis routes.[4] However, just very few publications analyze entire process chains for the production of $OME_{3\text{-}5}$. Recently, Schmitz et al.[11] investigated the economic potential of a process chain for the production of $OME_{3\text{-}5}$ from methanol. In order to include methanol also as a renewable feedstock, they consider a methanol price ranging from 100 US$/t to 500 US$/t, where the lower and upper limit reflect the price for methanol produced from natural gas and biomass, respectively.[11] The economic assessment is based on material balances assuming a yield of 100% for the trioxane, OME_1, and $OME_{3\text{-}5}$ plant and 88% for methanol towards FA. The energy demands for the isolated processes are either extrapolated from literature or assumed to be equal to similar processes within the chain. For the calculation of investment cost, a general costing model for refineries is used. Considering these process assumptions along with a low methanol price and low investment cost, $OME_{3\text{-}5}$ production using their benchmark process chain is found to be competitive with conventional diesel. Jacob and Maus[10] use the results to compare the process developed by Schmitz et al.[11] with the coal-based production process in China, a novel route by Schmitz et al.,[12] a perspective route using DME and FA, as well as with the production of OME_1. The coal-based production process and the perspective route was found to be cheaper by 16% and 45%, respectively. Also Ouda et al.[13] propose a process chain starting from methanol only. There, formaldehyde is being produced in a first reactor at high temperature by methanol dehydrogenation. This avoids the formation of water, such that its subsequent step, i.e.,

$OME_{3\text{-}5}$ synthesis, is based on a water-free feed. However, in this step, water is produced as a byproduct and shifts reaction equilibrium towards the educts. In a subsequent article, Ouda et. al[14] propose a detailed process concept including separation via distillation and evaluate its economic potential and its efficiency. However, process models used are rather simple and the proposed distillation sequence differ from other publications (e.g.,[12,15]). The same reaction to form $OME_{3\text{-}5}$ from methanol and formaldehyde is considered in a holistic evaluation of biomass-based $OME_{3\text{-}5}$ production by Zhang et al.[16,17] There, Aspen Plus® models for each process step have been implemented, the most relevant process parameters identified, and their influence on $OME_{3\text{-}5}$ yield analyzed. Mahbub et al.[8] extend this analysis by a life-cycle assessment taking into account biomass production, biomass transportation, chemical conversion, fuel mixing, fuel dispensing, and vehicle combustion. It is shown that the total life-cycle green house gas emissions can be reduced by up to 86% compared to fossil diesel.

The process efficiency, the economic competitiveness, as well as the GWI reduction potential for $OME_{3\text{-}5}$ production via formaldehyde and methanol has been assessed greatly in literature. In contrast to such an aqueous route, the hydrous one via trioxane and OME_1 is beneficial in the following: It avoids water formation, saves energy and unit operations for its removal, and shifts reaction equilibrium to $OME_{3\text{-}5}$. However, trioxane is known to be expensive to purchase and its conventional stand-alone production energy intensive.[18,19] By considering a novel trioxane process and integrating it into the entire value chain, these drawbacks do not necessarily hold anymore, as methanol and formaldehyde production is accompanied by significant steam generation. A concurrently submitted article[20] deals with corresponding analyses. Due to the benefits and just little detailed information in literature about $OME_{3\text{-}5}$ production starting from H_2 and CO_2 via trioxane and OME_1, we implement detailed models from literature using Aspen Plus® and conduct process simulations and analyses. This reveals the potential and limits of integrating trioxane production into the value chain, such that improvements for future production concepts can be derived system-

atically. We explicitly provide the implementations of process models in Aspen Plus® via our homepage,[21] which can be used as a basis for further OME analyses respecting some constraints and limits given in Section 4.1.2. Such model implementations including highly complex thermodynamics have not been published by anybody else before.

The article is organized as follows: Section 2 introduces the variety of different synthesis routes for $OME_{3\text{-}5}$ production by distinguishing between the aqueous and anhydrous ones. Corresponding benefits and challenges are discussed and the potential of the anhydrous route highlighted. Subsequently, in Section 3 both intermediate processes for the chain growth of OME_1, i.e., trioxane and $OME_{3\text{-}5}$ production, are described. Section 4 introduces the thermodynamic model used in this study, as well as its coupled reaction kinetics, and the unit operation models used in Aspen Plus®. The process results for the entire process chain are presented in Section 5, before Section 6 concludes the findings of this paper.

2 Synthesis Routes for $OME_{3\text{-}5}$ Production

As indicated in Figure 1, for the production of OME_n with different chain lengths two main elements need to be provided: methoxy groups and formaldehyde molecules. The former constitute the end groups of OME_n and may be taken from methanol, OME_1, or DME. The formaldehyde molecules for chain growth may be provided from aqueous or methanolic FA, paraformaldehyde (PF), or solid trioxane (TRI). The process analyzed in this work is solely based on H_2 produced from renewable energy and CO_2 from biomass, flues gas, or directly captured from air. The provision of these raw materials are not discussed on process level within this paper. Instead, they are considered in a concluding exergy efficiency analysis of the entire production process.

Figure 1 gives an overview of routes starting from the CO_2 sources air, biomass, and flue gas, as well as sources for H_2, i.e., water via electrolysis and biomass via gasification. A

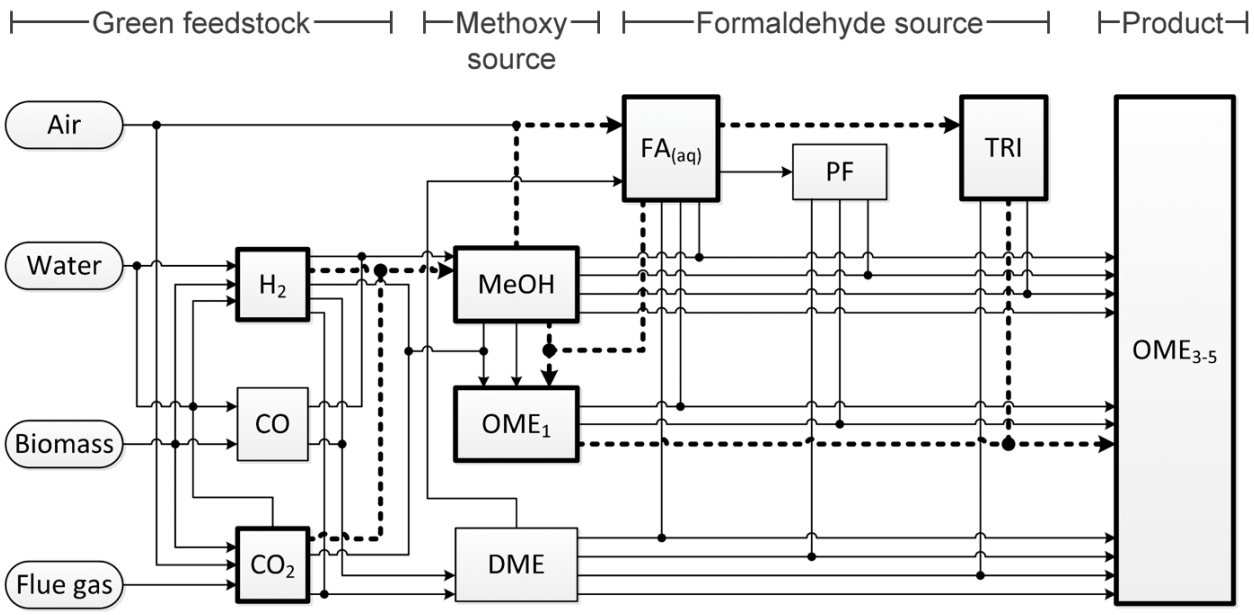

Figure 1: Flow diagram with possible synthesis routes for $OME_{3\text{-}5}$ production from renewable H_2 and green CO_2. The dashed, bold path corresponds to the anhydrous process chain considered in this work.

discussion of all these routes is out of the scope of this investigation. In order to provide a basis of information about the process steps affecting $OME_{3\text{-}5}$ directly, we focus on the synthesis reactions from different methoxy and formaldehyde sources. In general, all routes can be classified either as an anhydrous or aqueous synthesis route,[22] i.e., distinguishing whether water is formed in the $OME_{3\text{-}5}$ formation reaction or not.

Within the majority of currently discussed synthesis routes, water is produced as a byproduct, e.g., in the synthesis of $OME_{3\text{-}5}$ from methanol and aqueous FA (formalin). The synthesis of $OME_{3\text{-}5}$ from methanol and aqueous FA has recently received a lot of attention as only three process steps are involved: methanol, FA, and $OME_{3\text{-}5}$ production.[11,12,22–27] This is particularly promising in terms of capital costs and utility demand, which make this process route highly attractive for industrial production. However, its main shortcoming is the need for removing water, which is produced as a byproduct and additionally introduced into the system by the aqueous FA feed. The presence of water lowers the selectivity towards $OME_{3\text{-}5}$, as methylene glycols are formed in a competing reaction. Schmitz et al. recently published a process, where water is removed either by adsorption[12] or via membranes.[28]

The process concept has been proven feasible in lab-scale and is continuously improved in academia and industry.

By using PF instead of formalin, no water is introduced into the $OME_{3\text{-}5}$ synthesis. However, it is still produced stoichiometrically depending on the chain length distribution of PF.[29] Oestreich et al.[30] perform reaction equilibrium experiments using PF and methanol, coming to the conclusion that this reaction's obstacle is the formation of a significant amount of byproducts. For an innovative $OME_{3\text{-}5}$ production process they propose an extractive separation of OME with hydrocarbons yielding a high extraction selectivity. By exchanging methanol with OME_1 as the methoxy source, the reaction selectivity towards $OME_{3\text{-}5}$ increases significantly.[29,31–35] However, the production of PF from aqueous FA via vacuum distillation[36] requires several steps under various temperatures and is thus rather complex. Additionally, under given conditions PF is in solid state, which makes its handling challenging.

Utilizing trioxane as formaldehyde source the presence of water in $OME_{3\text{-}5}$ synthesis, and hence its complex removal, is truly avoided. In this regard, the production of $OME_{3\text{-}5}$ from OME_1 and trioxane is an intensively investigated process.[37–41] A corresponding process can be composed of comparatively simple unit operations and is characterized by its high selectivity towards $OME_{3\text{-}5}$: Selectivities of up to 70% are reported as well as a high stability of the catalyst's activity.[42–47] In contrast, some publications mention the high energy demand of the conventional trioxane production process and its high complexity.[19] Therefore, trioxane is often considered as an unfavorable and expensive intermediate in $OME_{3\text{-}5}$ synthesis.[18] However, it remains unclear whether these drawbacks still hold for a novel production process based on distillation,[48,49] which eventually benefits from heat integration with the entire value chain. This question is the subject of the following investigation.

The other synthesis routes indicated in Figure 1 (e.g., synthesis from DME[50–53]) are much less discussed in literature and, thus, no suitable data for detailed process analyses is available.

3 Process Description

The objective of part two of this two-part article is the evaluation of the anhydrous $OME_{3\text{-}5}$ production route starting from H_2 and CO_2. Special attention is given to the integrability of a promising trioxane process into the entire process chain and whether this overcomes the shortcomings of the conventional trioxane production. This analysis requires detailed process information, e.g., heat flows and temperature levels of all heat sinks and sources, as we perform a pinch-based heat integration. For formaldehyde containing processes it is essential to use detailed models as its reactive behavior influences such process characteristics significantly. Due to that, each of the process chain's five intermediate steps are modeled. Part one of our two-part article[54] introduces the processes for methanol, FA, and OME_1 production and is not discussed in further detail here. The two subsequent steps, i.e., trioxane and $OME_{3\text{-}5}$ production, are described in the following.

3.1 Trioxane Production Process

Conventionally, trioxane is synthesized from aqueous FA in a highly energy intensive process consisting of several intermediate steps including FA concentration, reaction, trioxane extraction, separation, and purification.[19] At least five columns and one reactor is necessary for these operations. The need for an entrainer adds a further variable to the process, thus, making optimal process design as well as operation a challenging task. Apart from the complex flowsheet design, the loss of FA is not negligible reaching a yield of about 88%. Furthermore, a steam demand of 14.5 kg/kg_{TRI}[19] is economically and ecologically disadvantageous. Due to the high complexity, high steam demand and rather low yield of the conventional trioxane production process, Grützner et al.[48] developed a novel process, in which separation is based on distillation only. The distillation regions of the ternary system FA, trioxane, and water are pressure dependent, which makes pressure swing distillation (PSD) a possible technology for trioxane separation. Only three columns at different pressure levels, one falling film

evaporator for concentrating the aqueous FA solution, and one reactor is necessary in order to produce trioxane with a negligible loss of FA (Figure 2). Thus, it is less complex, no entrainer is necessary, and a yield of almost 100% can be reached. These advantageous process characteristics make the concept highly interesting to be considered in a heat integrated process chain. However, no detailed information about its energy demand of the final process is reported in literature.

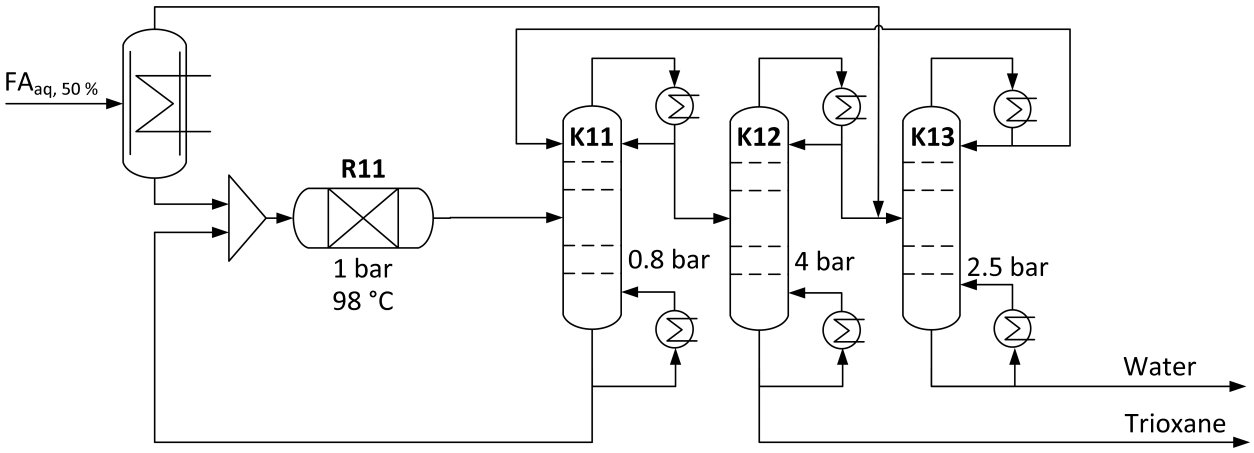

Figure 2: Distillation-based trioxane production with three columns at different pressure levels, one falling film evaporator, and one reactor at the conditions given by Grützner.[49]

The process specifications (Table 1) used in this work are based on the process given in Grützner et al.[48] and Grützner.[49] They are not optimized but chosen in such a way that technical feasibility is ensured and product purity is met. The flowsheet structure has been derived by an inf/inf-analysis.[55] Aqueous FA of approximately 50 wt.-% is fed into a falling film evaporator, where the solution is concentrated to up to 70 wt.-% FA, limited by precipitation. The concentrated solution is fed together with the bottom product of the first column K11, mainly consisting of water and unreacted FA, into reactor R11, in which the reaction to trioxane takes place using a sulfuric acid catalyst. The process model proposed by Grützner et al.[48] assumes the catalyst to either stay in the reactor or to be recycled with the bottom product of column K11. The reactor effluent, i.e., trioxane, FA, and water, is fed into column K11 and its overhead product into the next stage of the PSD sequence, i.e., column K12. Due to the pressure shift from 0.8 bar to 4 bar, technical trioxane can be withdrawn

as the bottom product with a purity of at least 99.9 wt.-%. The overhead product is mixed with the aqueous FA solution from the overhead product of the concentration unit, from which pure water is separated in the third stage of the PSD, i.e., column K13, at 2.5 bar. The overhead product is finally recycled to the first column K11. The process specifications are summarized in Table 1. Precipitation and crystallization of trioxane is not an issue since the process temperatures are higher than the melting point of trioxane, i.e., 62 °C, for all process streams. The good solubility of trioxane in water[56] as well as in ethers[36] makes the solid appearance of trioxane at ambient conditions not being obstructive for the process.

Table 1: Process specifications for the trioxane production process given by Grützner[49]

Variable	Value				
	Overall feed	R11	K11	K12	K13
Concentration	50 wt.-% FA	N/A	N/A	N/A	N/A
Pressure	1 bar	1 bar	0.8 bar	4 bar	2.5 bar
Temperature	N/A	98 °C	N/A	N/A	N/A
Top	N/A	N/A	85 °C	130 °C	115 °C
Bottom	N/A	N/A	93 °C	165 °C	127 °C
Stages	N/A	N/A	15	21	18
Feed stage	N/A	N/A	9	5	12
Mass reflux ratio	N/A	N/A	2.21	0.12	1.20
Mass distillate to feed ratio	N/A	N/A	0.045	0.905	0.900
Vapor fraction	N/A	0	N/A	N/A	N/A

3.2 $OME_{3\text{-}5}$ Production Process

For $OME_{3\text{-}5}$ production from trioxane and OME_1, the variety of process alternatives is small. Most of current research dealing with this synthesis route is about optimizing the catalytic reaction of trioxane and OME_1 to $OME_{3\text{-}5}$ in order to increase selectivity and con-

version.[42–45,47,57–59] Process-related literature is only known for the heterogeneously acidic catalyzed synthesis and a subsequent separation via distillation considered herein, as well as a homogeneously catalyzed synthesis. A series of patents, e.g.,[57,58] , investigates the homogeneously catalyzed production process consisting of three rectification columns, one reaction unit, and an extraction column. The catalyst, i.e., an ionic liquid, along with the extraction unit make this process more complex compared to the heterogeneously catalyzed one, which was developed by Burger[38] in an industrial-academic cooperation[60] and is shown in Figure 3. In this process, a mixture of trioxane and OME_1 is fed into reactor R21 together with a recycle stream coming from the bottom of column K22 and K23. The reaction in R21 takes place under moderate conditions and the reaction mixture consisting of unreacted trioxane, OME_1, $OME_{n>1}$, and undesired byproducts is fed into a sequence of columns. First, in column K21 unreacted educts, $OME_{n=2}$, and byproducts are separated from all OME_n with a chain length higher than two FA groups. Byproducts are separated from unreacted educts and purged through the distillate of column K22, while the bottom product is recycled into reactor R21. In column K23 the desired product $OME_{3\text{-}5}$ is isolated from OME_n with a chain length of higher than five FA groups.

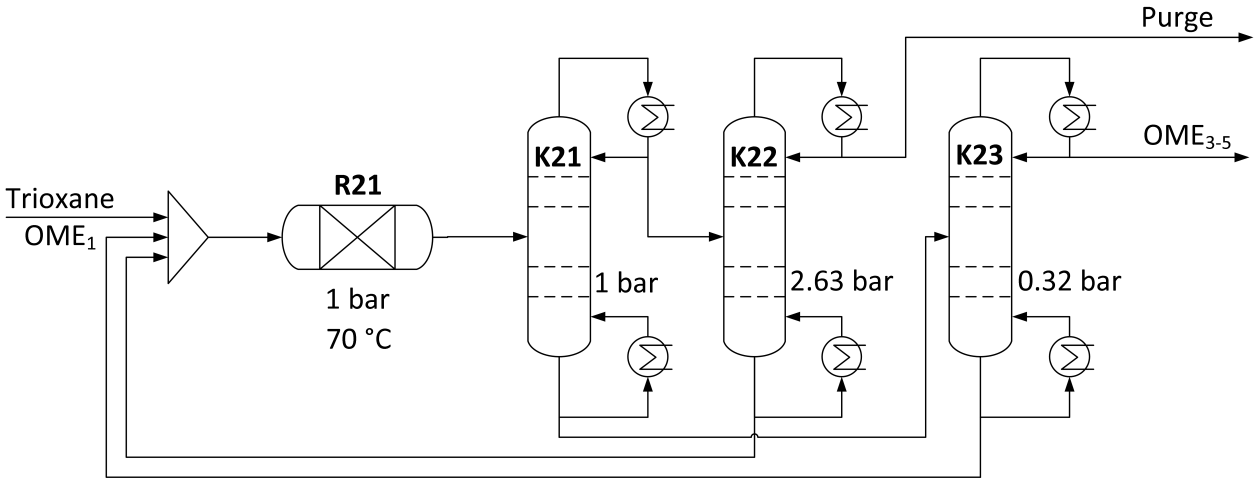

Figure 3: Distillation-based $OME_{3\text{-}5}$ production with three columns at different pressure levels and one reactor at moderate conditions given by Burger et al.[41]

Burger et al.[41] derived the structure of the flowsheet using the inf/inf-method[55] and op-

timized the unit specifications by a two-stage optimization procedure: First, the continuous variables, i.e., overall feed concentration and reflux ratios, were fixed and the discrete variables, i.e., number of stages and feed stage of each column, were varied in order to minimize each reboilers energy duty. Subsequently, the discrete variables were fixed and the continuous variables optimized w.r.t. minimal total reboiler duty using a gradient based method. Both steps were performed iteratively until the optimal unit specifications given in Table 2 were found. We increased the number of stages in all columns in order to reach the reboiler duties given by Burger et al.[41]

Table 2: Process specifications for the $OME_{3\text{-}5}$ production process given by Burger et al.[41] The stage specifications have been adjusted in order to meet product specifications

Variable	Value				
	Overall feed	R21	K21	K22	K23
Concentration	51.6 wt.-% Trioxane	N/A	N/A	N/A	N/A
Pressure	1 bar	1 bar	1 bar	2.63 bar	0.32 bar
Temperature	N/A	70 °C	N/A	N/A	N/A
Top	N/A	N/A	50 °C	18 °C	134 °C
Bottom	N/A	N/A	186 °C	83 °C	250 °C
Stages	N/A	N/A	30	30	15
Feed stage	N/A	N/A	3	31	4
Mass reflux ratio	N/A	N/A	0.048	9.700	0.215
Mass distillate to feed ratio	N/A	N/A	0.535	0.00066	0.683
Vapor fraction	N/A	0	N/A	N/A	N/A

4 Model Description

All process simulations performed in this work are built on thermodynamic and chemical reaction models from literature, which are implemented in Aspen Plus®. The models of the first three process steps, i.e., methanol, formaldehyde, and OME_1 production, are covered in

part one of our two-part article.[54] Overlapping models are not repeated hereinafter. Instead, Section 4 complements part one of the two-part article by providing all additional information about the thermodynamic and chemical reaction models relevant for the trioxane and $OME_{3\text{-}5}$ processes only. For modeling the trioxane process, the thermodynamic system of a mixture containing water and FA coupled with its oligomerization reactions to polyoxymethylene glycols (MG) are essential. In this regard, we extend the model described in part one with parameters for trioxane and OME_n with a chain length of up to 20 FA groups in order to account for all relevant phenomena happening within trioxane and $OME_{3\text{-}5}$ production. We collected these extensions from literature, combined them with the model used in Bongartz et al.,[54] and describe them in the following.

4.1 Chemical Reaction Model

The commonly assumed chain growth mechanism for OME_n synthesis is its reaction with one FA molecule:[61]

$$OME_{n-1} + FA \overset{H^+}{\longleftrightarrow} OME_n \quad (n \geq 2) \cdot \tag{R1}$$

This reaction only takes place under acidic conditions[26] and if monomeric FA is present. In the considered process chain, FA is provided by trioxane, which decomposes over an acidic catalyst to three FA molecules via the overall (not elementary) reaction

$$\text{Trioxane} \overset{H^+}{\longleftrightarrow} 3\ FA \cdot \tag{R2}$$

It may also be possible that the cyclic structure of trioxane brakes only at one point, such that a chain of three FA groups are incorporated directly in one OME_n molecule:[37]

$$OME_{n-3} + \text{Trioxane} \overset{H^+}{\longleftrightarrow} OME_n \quad (n > 3) \cdot \tag{R3}$$

However, experiments did not show any evidence for this mechanism,[37] so that the mechanism involving Reactions (R1) and (R2) is used in this work.

Trioxane itself is produced in a previous step, often described as the reverse of Reaction (R2), where FA is present in an aqueous solution. The presence of water makes the reaction system highly complex as FA and water instantaneously react to polyoxymethylene glycols even without the presence of any catalyst:[62]

$$\mathrm{H_2O + FA \longleftrightarrow MG_1} \tag{R4}$$

$$\mathrm{MG_{n-1} + FA \longleftrightarrow MG_n} \quad (\mathrm{n} > 1)\,. \tag{R5}$$

Therefore, monomeric FA is present in the system only at very low concentration, but is rather embedded and provided via MG. This makes trioxane formation according

$$\mathrm{MG_3 \overset{H^+}{\longleftrightarrow} Trioxane + H_2O} \tag{R6}$$

much more probable.[63,64] The oligomerization reactions also play a governing role in the synthesis of FA within this process chain, which is discussed in further detail in Bongartz et al.[54]

In addition to the desired Reactions (R1) and (R2) for $\mathrm{OME_{3\text{-}5}}$ production, some side reactions may occur under specific conditions. FA can react to methyl formate (MF) via the Tischenko reaction (R7).[65] This reaction also takes place under acidic conditions and favorably at temperatures above 90 °C when using Amberlyst 46 as a catalyst.[39] The same holds for the decomposition of $\mathrm{OME_1}$ to DME and FA according to Reaction (R8).

$$\mathrm{2\ FA \xrightarrow{H^+} MF} \tag{R7}$$

$$\mathrm{OME_1 \xrightarrow{H^+} DME + FA} \tag{R8}$$

How these reactions were accounted for in the simulations and how they were implemented in Aspen Plus® is described in Section 4.1.1 and 4.1.2 for the trioxane and $OME_{3\text{-}5}$ production, respectively. The model implementations in Aspen Plus® are available via our homepage.[21]

4.1.1 Conversion-based Model for Trioxane Production

Whereas the oligomerization reactions of water and FA to MG are investigated extensively in literature,[66–70] comparably little information is available about the formation of trioxane from aqueous FA. Grützner[49] performed several experiments in order to derive temperature dependent correlations for the equilibrium and reaction rate constants of Reactions (R6) and (R7). However, corresponding parameter sets are not given. Therefore, the simulation for the trioxane production process in this work is based on the reaction mechanism according to Reaction (R6) with a once-through conversion of 5% trioxane, which is a typical value for industrial trioxane production.[48] Side reactions are neglected as the concentrations of relevant components are low.[48]

In contrast to the desired formation of trioxane, which takes place only within the catalytic region of the reactor, the oligomerization reactions of FA and water to MG take place in all units. Therefore, the corresponding equilibrium model[67] is implemented in each stage of the columns, all mixers and splitters, as well as in the reactor. The adaption and implementation of this model in Aspen Plus® is described in Bongartz et al.[54]

4.1.2 Reaction Kinetic Model for $OME_{3\text{-}5}$ Production

The $OME_{3\text{-}5}$ production process is based on the model developed by Burger et al.[39] All parameters have been derived for the reaction system consisting of Reactions (R1) and (R2), which are catalyzed heterogeneously by the catalyst Amberlyst 46. In contrast to the oligomerization reactions (R4) and (R5), OME_n formation only takes place in the presence of a catalyst. Therefore, these reactions are accounted for only in the reactor. As the byproduct methyl formate is formed in small amounts in Reaction (R7) and influences process design,

an equation describing this reaction formally was added to the chemical reaction model (cf., Burger et al.[41]). Burger et al.[39] suggest a reaction model using a modified Langmuir-Hinshelwood-Hougen-Watson (LHHW) approach, as the sorption processes were found to be rate limiting. However, the simulation software Aspen Plus® does not allow the application of such a model, so that the pseudohomogeneous kinetic model discussed in Burger et al.[39] is used in a slightly modified way in this work. Burger et al.[39] show that this model is not able to produce consistent results for a varying feed composition. The adaption of the reaction rate parameters for Reaction (R2), however, makes the model applicable for the optimal operating point found by Burger et al.[41] only. The set of parameters for the mole fraction-based equilibrium constants used in this work is given in Table (S1) of the supplemental information (SI) and only applicable for this operating point using Amberlyst 46 as the catalyst. Corresponding parameter sets for the rate constants are given in Table (S2) of the SI. Parameters for the formation of methyl formate are estimated in order to reach a formation rate of 0.02 kg/(h kg_{cat}).[41] All constants for OME_n with different chain lengths are assumed to be equal and for trioxane decomposition the kinetic parameters were adjusted in order to fit the results given at the optimal operating point stated in Burger et al.[41] This adjustment is necessary as the pseudohomogeneous kinetic model is not applicable for arbitrary feed compositions.[39]

4.2 Thermodynamic Model

The thermodynamic model for $OME_{3\text{-}5}$ production corresponds to the one given in the work of Burger et al.[41] and is presented for pure and mixture properties hereinafter. Property models for FA and trioxane containing aqueous solutions used in this series of papers are taken from Albert[67] and Ott.[71]

4.2.1 Pure Component Properties

Correlations for the pure component properties were implemented for MG and $OME_{n>1}$. For the rest of the pure components, i.e., water, methanol, FA, trioxane, MF, and OME_1, correlations were used from the APV88 Pure32 Aspen database. They constitute liquid molar density $\rho_{L,i}$, ideal heat capacity c_p^{ig}, vapor pressure p_i^s, and heat of vaporization $\Delta h_{v,i}$.

4.2.2 Mixture Properties

In order to account for nonideal interactions between all species, the UNIFAC group contribution method[72] is used as the basis for estimating all activity coefficients. For the trioxane production process, the UNIFAC approach is applied directly using corresponding UNIFAC-groups defined by Albert et al.,[66] whereas the $OME_{3\text{-}5}$ production process uses the NRTL[73] approach based on data produced by the UNIFAC method. Burger et al.[41] fitted NRTL coefficients to the UNIFAC estimations for the binary systems constituting FA, trioxane, OME_1, $OME_{n>1}$, and MF. For the binary system OME_2 and trioxane, the activity coefficients were fitted to experimental data given by Burger et al.[41] using the global parameter estimation tool BOARPET.[74–76]

4.3 Process Models

In order to reach high accuracy, detailed unit operation models are used within the Aspen Plus® model implementations. For the distillation columns, this is particularly important as oligomerization reactions need to be taken into account explicitely. Therefore, both process models, i.e., trioxane and $OME_{3\text{-}5}$ production, constitute rigorous RadFrac models for separation operations only. The Newton solution algorithm has shown best results in terms of convergence and is used for all RadFrac models. As packing specifications, column dimensions, and pressure drop specifications are given for the distillation columns of the $OME_{3\text{-}5}$ production process in the work of Burger et al.,[41] those have been considered in this work as well. Due to limited information about the distillation columns in the trioxane produc-

tion process, they are modeled using an equilibrium calculation type. The conversion-based reaction of aqueous FA to trioxane is modeled using a RStoic reactor. Due to the given kinetics for the $OME_{3\text{-}5}$ process, reactions take place in a RPlug reactor with specifications given in the work of Burger et al.[41] Compressors are isentropic and all unit operations consider oligomerization reactions given in Equation (R4) and (R5). Flowsheet tear streams are calculated using the Wegstein convergence method with a default relative tolerance of $1x10^{-4}$.

5 Results and Discussion

Detailed mass balances for the trioxane and $OME_{3\text{-}5}$ production process steps can be found in the work of Grützner[49] and Burger et al.,[41] respectively. We address herein the overall material (Section 5.1) and utility demand (Section 5.2) of each intermediate process step, as well as the entire production chain. Special attention is given to the integrability of the distillation-based trioxane process, as its conventional stand-alone production is known to be energy-intensive and expensive. This enables a holistic and rational evaluation of the anhydrous $OME_{3\text{-}5}$ production and provides a further basis for fair process comparisons.

5.1 Material Demand for $OME_{3\text{-}5}$ Production

Following the process chain for OME_1 production presented by Bongartz et al.,[54] which is part of this works process, H_2 and CO_2 is consumed solely by the methanol production plant. For 1 kg $OME_{3\text{-}5}$, 0.25 kg H_2 and 1.83 kg CO_2 is needed to produce 1.28 kg methanol as illustrated in Figure 4. In accordance with the simulations conducted by Burger et al.,[41] the composition of $OME_{3\text{-}5}$ is assumed to be 43 wt.-% OME_3, 34 wt.-% OME_4, 22 wt.-% OME_5, and 1 wt.-% OME_6 in this study. As depicted in Figure 4, more than 50% of the consumed raw materials constitute air for the combustion in the methanol and FA production processes. In the FA production process, this corresponds to a high amount of inert gases

and keeps its operation beyond explosive limits. Apart from 2.14 kg air and 0.86 kg methanol about 0.40 kg water is fed into the FA process in order to absorb the FA molecules from the gaseous reactor effluent. This way 1.45 kg aqueous formaldehyde solution with 50 wt.-% FA is produced and 1.95 kg exhaust gas released to the atmosphere. In the subsequent steps more than 73% of the FA solution is used for trioxane production and the remaining 27% for OME_1 production. In both processes, water needs to be separated from both products, which are present in about the same quantity. In the last process the chain growth of OME_1 to $OME_{3\text{-}5}$ takes place with an overall carbon-based yield of almost 100%: 0.48 kg OME_1 reacts with 0.52 kg trioxane to 1 kg $OME_{3\text{-}5}$. Only 0.001 kg of an equimolar mixture containing FA and MF need to be purged in order to prevent MF accumulation. However, as the corresponding material stream is comparably small, it is neglected in the diagram in Figure 4.

The *chemical conversion efficiency* (cf., e.g., König et al.[77])

$$\eta_{\mathrm{CCE}} = \frac{\dot{m}_{\mathrm{OME_{3-5}}} \cdot \mathrm{LHV}_{\mathrm{OME_{3-5}}}}{\dot{m}_{\mathrm{H_2}} \cdot \mathrm{LHV}_{\mathrm{H_2}}}, \tag{1}$$

of this process chain is 63%, considering a lower heating value (LHV) of 121.84 MJ/kg_{H_2} and 19.16 $MJ/kg_{OME_{3\text{-}5}}$ for H_2 and $OME_{3\text{-}5}$, respectively. Concerning the amount of CO_2 required for producing 1 kg $OME_{3\text{-}5}$, an overall carbon-based yield of 87% is reached.

5.2 Energy Demand for $OME_{3\text{-}5}$ Production Considering Heat Integration

The main objective of this paper is the evaluation of an entirely heat integrated process chain for the anhydrous production of $OME_{3\text{-}5}$ from H_2 and CO_2 utilizing a novel trioxane process. In this regard, two different cases for heat integration are distinguished: In the first case, heat integration is considered for each intermediate process separately from the other processes and only remaining excess heat, i.e., steam that is commonly generated in

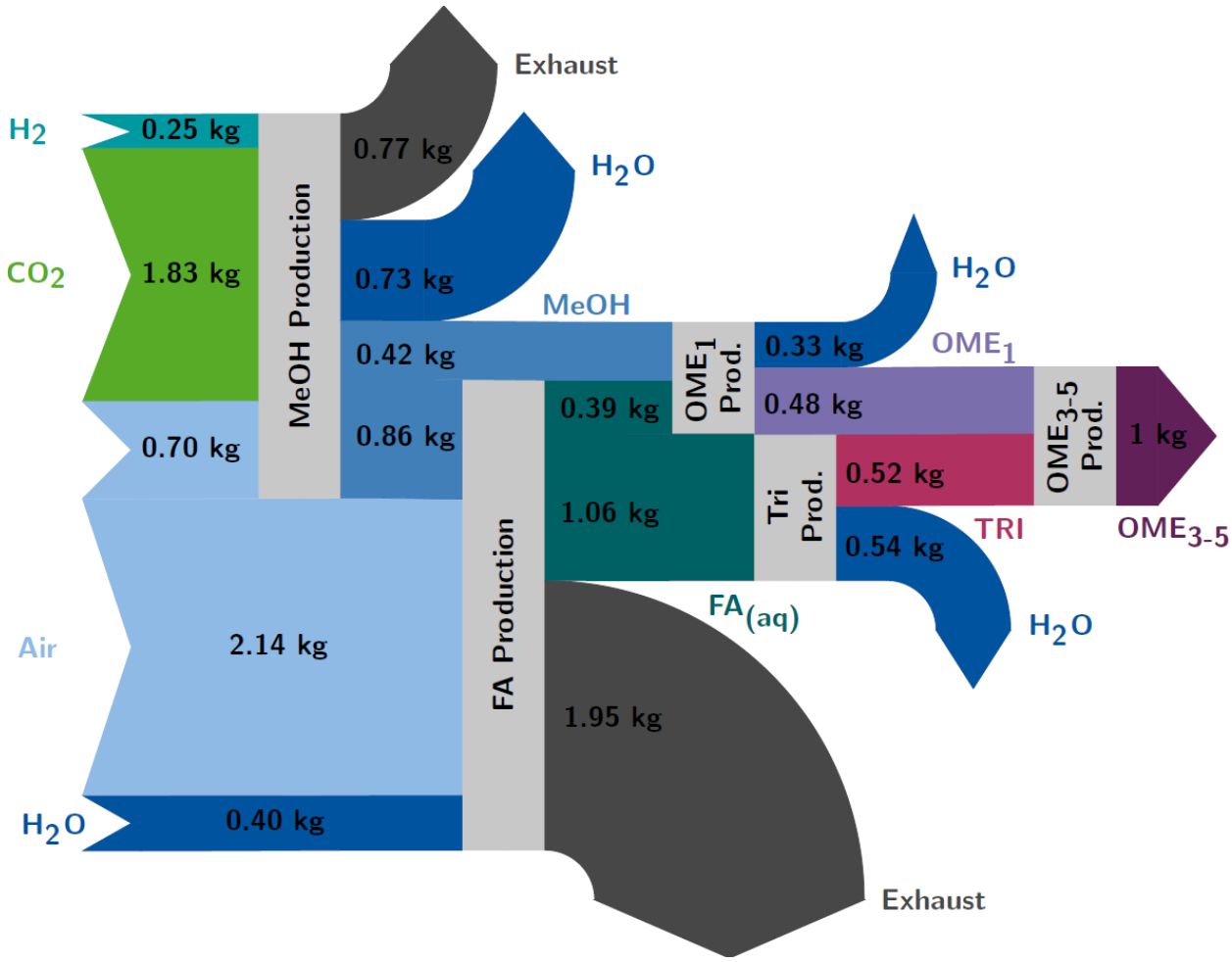

Figure 4: Material flows within the reference process chain for the production of 1 kg $OME_{3\text{-}5}$.

methanol and FA production, is assumed to be used in the other process steps. In the second case, heat integration is conducted considering all heat sources and sinks within the process chain simultaneously. In both cases a targeting approach using pinch analysis is conducted. This way, an energetically best case process chain with respect to energy integration is found, which, however, does not necessarily represent the economic optimum as no rigorous heat exchanger network is developed. In order to estimate the influence of the process performance of trioxane production on the overall one, a sensitivity analysis is performed. Regarding this, FA conversion towards trioxane is varied and the heat demand of the heat integrated process calculated. This reveals potential improvements of the anhydrous $OME_{3\text{-}5}$ production, if the catalytic trioxane reaction can be further optimized.

We assume that H_2 is provided by a proton exchange membrane (PEM) electrolysis operated at 30 bar. CO_2 may be captured from biogas plants, from flue gas of power plants, or directly from air and is fed into the methanol production plant at ambient conditions. As for the direct conversion of methanol from H_2 and CO_2 an operating pressure of about 70 bar is necessary,[78] the energy demand for the compression of both educts are considered. For CO_2, a four stage compression including intercooling is applied and for H_2 only one stage. This way a total electricity consumption of 1.33 $MJ/kg_{OME_{3\text{-}5}}$ for pumping and compression need to be provided for the methanol plant (Figure 5). The heat demand for heat exchanger and distillation columns is entirely covered by the heat of reaction and combustion within the process itself. The same holds for the FA production process, so that excess heat of 1.76 $MJ/kg_{OME_{3\text{-}5}}$ at about 220 °C and 5.01 $MJ/kg_{OME_{3\text{-}5}}$ at about 150 °C is available for subsequent processes. About 0.16 $MJ/kg_{OME_{3\text{-}5}}$ for compression is necessary in the FA production process to maintain a steady flow of materials. For OME_1 production, the energy demand for pumping and compression can be neglected as only comparably low pressure levels are necessary and the streams are comparatively small and liquid. Therefore, 4.25 $MJ/kg_{OME_{3\text{-}5}}$ heat needs to be provided for separating OME_1 from methanol and water, that may be taken

from either the excess heat of the FA process entirely, or partly from the methanol and FA process. If the second option is chosen, the remaining heat of the FA process may be used for trioxane production.

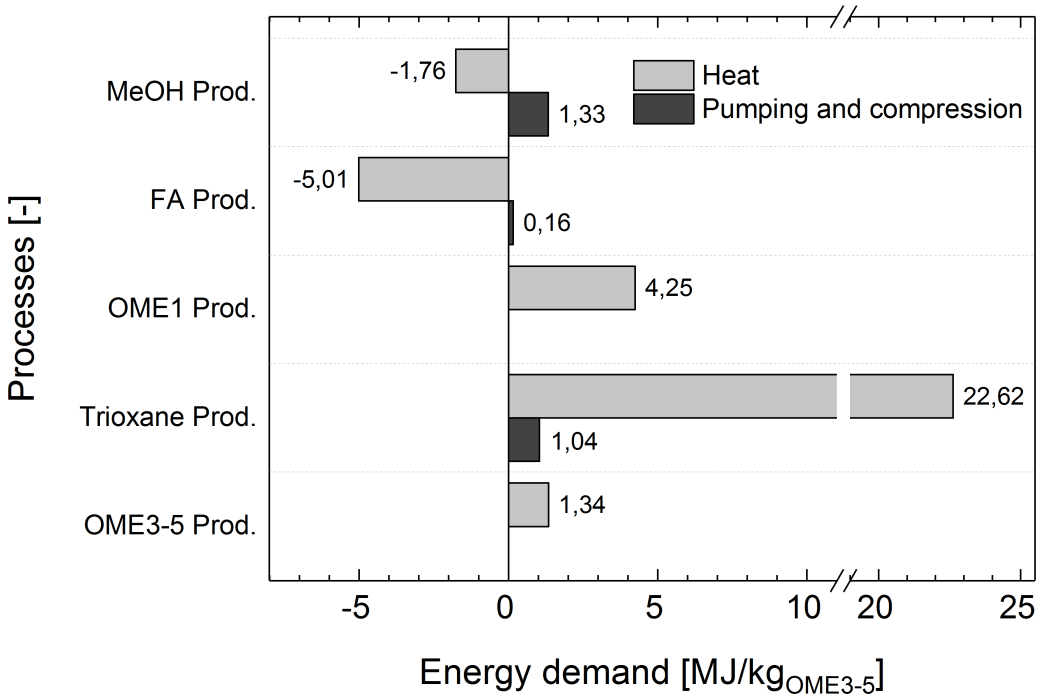

Figure 5: Energy demand for heating as well as pumping and compression of the processes within the reference $OME_{3\text{-}5}$ production chain. Heat integration is considered within each individual process.

The trioxane production process consumes in total 22.62 $MJ/kg_{OME_{3\text{-}5}}$ considering internal heat integration, which is about 15 kg/kg_{TRI} steam and in accordance with the steam demand of the conventional trioxane production process given in the work of Mahieux.[19] Grützner[49] reports a heat demand for the distillation-based trioxane production process of about 65 MJ/kg_{TRI}, which is about 33.70 $MJ/kg_{OME_{3\text{-}5}}$. This is considerably higher than found in this work as no heat integration is considered in his work. The high demand of heat is mainly caused by a small conversion of 5% of FA to trioxane in the reactor, which results in a high recycle stream leaving the bottom of column K11 and, thus, in a high energy demand for its reboiler. As a conversion of 5% is only a reference value for conven-

tional industrial applications,[48] its influence on the energy demand of the separately heat integrated trioxane production process and on the process chain's one is illustrated in Figure 6. The diagram shows a strong relation between FA conversion and the heat demand of the trioxane production process: Heat demand for trioxane production halves by considering a FA conversion of 10% instead of 5%. The energy demand of the overall process chain is smaller than that of the separately heat integrated trioxane process, because excess steam from formaldehyde production is utilized. In addition to heat, 1.04 $MJ/kg_{OME_{3-5}}$ electricity

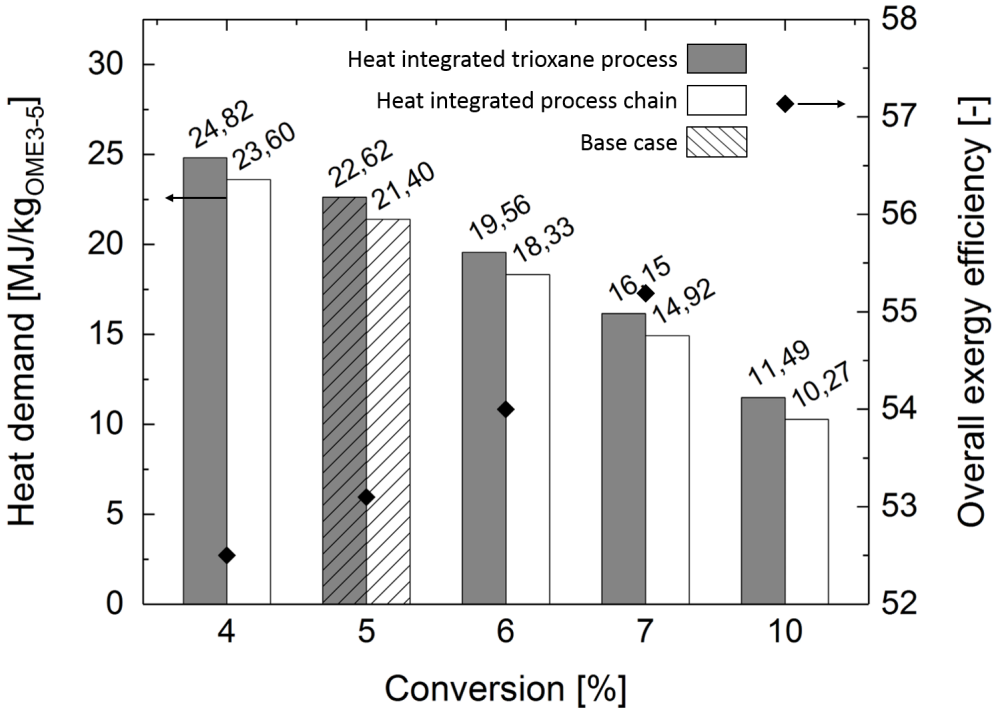

Figure 6: Influence of the conversion of FA to trioxane on the energy demand of the separately heat integrated trioxane production process, as well as on the overall energy demand of the entire process chain. Additionally, the exergy efficiency of the overall process chain starting from H_2 and CO_2 is shown.

for compression need to be provided, as the gaseous overhead product of column K11 need to be fed into the second column K12 operated at 4 bar. However, this way heat for internal heat integration is produced. As the energy demand for trioxane production exceeds the energy demand of the other processes within the process chain by a large amount, the overall energy efficiency is highly dependent on this process step. However, the process for

trioxane production investigated in this study was not optimized rigorously and, thus, still offers potential for improvements.

The energy demand for the heat integrated $OME_{3\text{-}5}$ production process from trioxane and OME_1 is rather low with 1.34 $MJ/kg_{OME_{3\text{-}5}}$ at 200 °C to 260 °C for separating the product from $OME_{n<3}$, methyl formate, unreacted trioxane, and $OME_{n>5}$. Energy for pumping and compression can be neglected, as it is much lower than the electricity demand of the aforementioned processes. These results are in agreement with those from Burger et al.[41]

Given all material streams entering and leaving each process together with the processes energy demand and temperature levels, all exergy fluxes within the process chain for $OME_{3\text{-}5}$ production were calculated (cf., part one of our two-part article[54]) and are illustrated in the Sankey diagram in Figure 7. As CO_2 is provided at 1 bar and its chemical exergy is neglected, it does not bring any exergy into the system. Only a large exergy stream associated with the stream of H_2 at 30 bar and some electricity enter the process as input streams of the methanol production plant. Its exergy efficiency is calculated to be about 90%. If raw material compression is not considered as part of the methanol process, for example in case H_2 and CO_2 are provided from high-pressure storage sites, its exergetic efficiency increases to 91%. For the FA and OME_1 production plant, only electricity need to be provided externally as excess heat is assumed to be exchanged between the processes within the production chain. The exergy efficiency for these processes is 73% and 90%, respectively. The low efficiency of the FA production process is caused by irreversibilities during methanol combustion and the residual heat of exhaust gases (cf., Bongartz et al.[54]). As already mentioned above, the trioxane production process consumes most of the energy within the reference process chain, of which most is consumed in the reboiler of column K11. This makes the exergy efficiency of this step drop to about 55%. Considering the conversion of FA towards trioxane to be 10% instead of 5% its efficiency increases to 66% and the overall process chain efficiency to

more than 57% (cf., Figure 6). The most exergy efficient process for OME_{3-5} production is its last step, i.e., the chain growth of OME_1 to OME_{3-5}. As just little heat and electricity need to be provided to the process, its exergy efficiency reaches almost 97%. All in all, considering a system boundary around the entire reference process chain, the overall exergy efficiency for OME_{3-5} production from renewable H_2 and green CO_2 is 53%. Considering 10% FA conversion the efficiency increases to 57%.

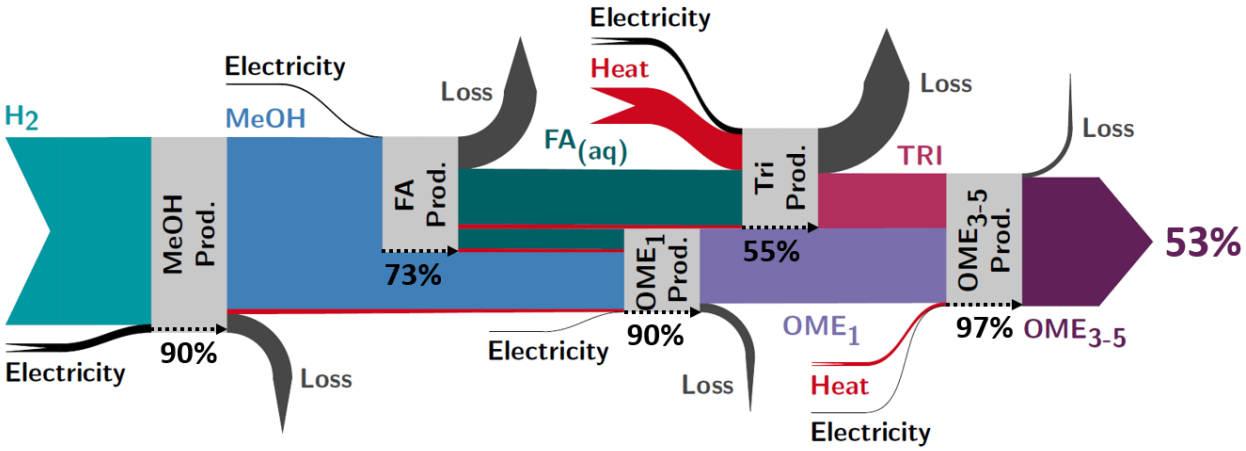

Figure 7: Sankey diagram of exergy flows within the reference process chain for the production of 1 kg OME_{3-5}. The gray boxes denote the different process steps and the percentages are the exergy efficiencies of these separate steps. The overall exergy efficiency from H_2 to OME_{3-5} is 53%

For the case where all process steps are at the same site, a more efficient combination of heat streams is possible and the overall exergy efficiency increases to 54%. The overall heat demand reduces by about 16% from 21.40 $MJ/kg_{OME_{3-5}}$ to 17.94 $MJ/kg_{OME_{3-5}}$. Assuming 4.5 kWh/Nm^3, i.e., 180 MJ/kg_{H_2}, for an alkaline electrolyzer with an HHV-based efficiency of about 80% and a maximum operating pressure of 32 bar,[79] 45 $MJ/kg_{OME_{3-5}}$ need to be provided only for hydrogen supply. The resulting overall exergy efficiency including H_2 supply via electrolysis is about 40%. Using PEM electrolyzers the overall efficiency is comparable as their specific energy consumption is about the same.[80] Including also a thermal energy demand of 2.20 MJ/kg_{CO_2} for carbon capture from flue gas with a typical carbon dioxide mole fraction of 13%[81] reduces the overall efficiency to 38%. This efficiency is rather low

compared to OME_1 production and other e-fuels. Even the best possible heat integration of the trioxane process within the entire process chain increases the total efficiency including electrolysis and carbon capture by only less than 1%. Finally, a potential optimization of the catalytic reaction of FA towards trioxane has a significant effect on the overall process performance. However, such improvements are also limited, e.g., doubling the FA conversion corresponds to an increase in overall process efficiency of only 2% starting from electricity. Despite an effective heat integration of the novel trioxane process in the entire process chain and a highly attractive final process step (i.e., $OME_{3\text{-}5}$ formation), from an energy point of view it is not expedient to further improve the synthesis of $OME_{3\text{-}5}$ via OME_1 and trioxane. Due to only small improvements for the entire process chain, even for a significantly improved catalytic trioxane reaction, the focus of future $OME_{3\text{-}5}$ research should be placed to alternative trioxane production processes or routes avoiding trioxane production.

6 Conclusion

Key for a successful development of a resource efficient $OME_{3\text{-}5}$ production process is the identification of bottlenecks established process concepts suffer from. In this work, such an analysis has been conducted for the anhydrous synthesis pathway of $OME_{3\text{-}5}$ starting from H_2 and CO_2 producing methanol, formaldehyde, OME_1, and trioxane as intermediates. For all of these process steps, simulations in Aspen Plus® have been performed using detailed process models with validated thermodynamic and chemical reaction models embedded. They were analyzed with respect to their material and energy demand, and ultimately evaluated using exergy efficiencies. For the production of 1 kg $OME_{3\text{-}5}$ with 43 wt.-% OME_3, 34 wt.-% OME_4, 22 wt.-% OME_5, and 1 wt.-% OME_6 0.25 kg H_2 and 1.83 kg CO_2 need to be provided. This corresponds to an overall carbon-based yield of 87% and a *chemical conversion efficiency* of 63%. The exergy efficiency of a heat integrated process chain considering the exchange of steam adds up to 53% starting from H_2 and CO_2. Including electricity and

thermal energy demand for electrolysis and carbon capture it drops to 38%. This efficiency is comparable to that of Fischer-Tropsch diesel or methanol-to-gasoline concepts based on renewable resources which have an overall efficiency of about 45% and 39%,[82] respectively, (assuming 80% efficiency for electrolysis). Taking into account that the trioxane production process is responsible for major exergy losses, the possibility for novel process concepts of avoiding this energy intensive process step, e.g., by the direct conversion of methanol and formaldehyde to $OME_{3\text{-}5}$, points towards the important areas for process improvements for $OME_{3\text{-}5}$ production. This is the focus of current research, e.g.,[12,28] , and need to be investigated in further detail in order to expand our analyses to such process concepts.

Acknowledgement

The authors gratefully acknowledge funding by the German Federal Ministry of Education and Research (BMBF) within the Kopernikus Project P2X: Flexible use of renewable resources – exploration, validation and implementation of 'Power-to-X' concepts. The authors also thank Philipp R. Dürr for his support in conducting the simulations.

Supporting Information Available

Tables of parameters for the chemical and thermodynamic model. VLE validation of a system containing trioxane and OME_2.

References

(1) Bongartz, D.; Doré, L.; Eichler, K.; Grube, T.; Heuser, B.; Hombach, L. E.; Robinius, M.; Pischinger, S.; Stolten, D.; Walther, G.; Mitsos, A. Comparison of light-duty transportation fuels produced from renewable hydrogen and green carbon dioxide. *Applied Energy* **2018**, *231*, 757–767.

(2) Schemme, S.; Samsun, R. C.; Peters, R.; Stolten, D. Power-to-fuel as a key to sustainable transport systems–An analysis of diesel fuels produced from CO_2 and renewable electricity. *Fuel* **2017**, *205*, 198–221.

(3) Härtl, M.; Gaukel, K.; Pélerin, D.; Wachtmeister, G. Oxymethylenether als potenziell CO_2-neutraler Kraftstoff für saubere Dieselmotoren Teil 1: Motorenuntersuchungen. *MTZ-Motortechnische Zeitschrift* **2017**, *78*, 52–59.

(4) Baranowski, C. J.; Bahmanpour, A. M.; Kröcher, O. Catalytic synthesis of polyoxymethylene dimethyl ethers (OME): A review. *Applied Catalysis B: Environmental* **2017**,

(5) Sirman, M. B.; Owens, E. C.; Whitney, K. A. *Emissions comparison of alternative fuels in an advanced automotive diesel engine*; 1998.

(6) Lautenschütz, L.; Oestreich, D.; Seidenspinner, P.; Arnold, U.; Dinjus, E.; Sauer, J. Physico-chemical properties and fuel characteristics of oxymethylene dialkyl ethers. *Fuel* **2016**, *173*, 129–137.

(7) Iannuzzi, S. E.; Barro, C.; Boulouchos, K.; Burger, J. POMDME-diesel blends: Evaluation of performance and exhaust emissions in a single cylinder heavy-duty diesel engine. *Fuel* **2017**, *203*, 57–67.

(8) Mahbub, N.; Oyedun, A. O.; Kumar, A.; Oestreich, D.; Arnold, U.; Sauer, J. A life cycle assessment of oxymethylene ether synthesis from biomass-derived syngas as a diesel additive. *Journal of Cleaner Production* **2017**, *165*, 1249–1262.

(9) Liu, H.; Wang, Z.; Zhang, J.; Wang, J.; Shuai, S. Study on combustion and emission characteristics of Polyoxymethylene Dimethyl Ethers/diesel blends in light-duty and heavy-duty diesel engines. *Applied energy* **2017**, *185*, 1393–1402.

(10) Jacob, E.; Maus, W. Oxymethylenether als potenziell CO_2-neutraler Kraftstoff für saubere Dieselmotoren Teil 2: Erfüllung des Nachhaltigkeitsanspruchs. *MTZ-Motortechnische Zeitschrift* **2017**, *78*, 54–61.

(11) Schmitz, N.; Burger, J.; Ströfer, E.; Hasse, H. From methanol to the oxygenated diesel fuel poly (oxymethylene) dimethyl ether: An assessment of the production costs. *Fuel* **2016**, *185*, 67–72.

(12) Schmitz, N.; Strofer, E.; Burger, J.; Hasse, H. Conceptual design of a novel process for the production of poly (oxymethylene) dimethyl ethers from formaldehyde and methanol. *Industrial & Engineering Chemistry Research* **2017**, *56*, 11519–11530.

(13) Ouda, M.; Mantei, F.; Elmehlawy, M.; White, R.; Klein, H.; Fateen, S.-E. Describing oxymethylene ether synthesis based on the application of non-stoichiomsetric Gibbs minimisation. *Reaction Chemistry & Engineering* **2018**, *3*, 277–292.

(14) Ouda, M.; Mantei, F.; Hesterwerth, K.; Bargiacchi, E.; Klein, H.; White, R. J. A hybrid description and evaluation of oxymethylene dimethyl ethers synthesis based on the endothermic dehydrogenation of methanol. *Reaction Chemistry & Engineering* **2018**, *3*, 676–695.

(15) Ai, Z.-J.; Chung, C.-Y.; Chien, I.-L. Design and control of poly (oxymethylene) dimethyl ethers production process directly from formaldehyde and methanol in aqueous solutions. *IFAC-PapersOnLine* **2018**, *51*, 578–583.

(16) Zhang, X.; Oyedun, A. O.; Kumar, A.; Oestreich, D.; Arnold, U.; Sauer, J. An optimized process design for oxymethylene ether production from woody-biomass-derived syngas. *Biomass and Bioenergy* **2016**, *90*, 7–14.

(17) Zhang, X.; Kumar, A.; Arnold, U.; Sauer, J. Biomass-derived oxymethylene ethers as diesel additives: A thermodynamic analysis. *Energy Procedia* **2014**, *61*, 1921–1924.

(18) Hackbarth, K.; Haltenort, P.; Arnold, U.; Sauer, J. Recent Progress in the Production, Application and Evaluation of Oxymethylene Ethers. *Chemie Ingenieur Technik* **2018**, *90*, 1520–1528.

(19) Mahieux, J. Make Trioxane Continuously. *Hydrocarbon Processing, International Edition* **1969**, *48*, 163.

(20) Held, M.; Tönges, Y.; Pélerin, D.; Härtl, M.; Wachtmeister, G.; Burger, J. On the energetic efficiency of producing polyoxymethylene dimethyl ethers from CO 2 using electrical energy. *Energy & Environmental Science* **2019**,

(21) Burre, J.; Bongartz, D. AspenPlus implementations of process models for the production of OME_n from H_2 and CO_2. `http://permalink.avt.rwth-aachen.de/?id=661625`, 2019.

(22) Ouda, M.; Yarce, G.; White, R.; Hadrich, M.; Himmel, D.; Schaadt, A.; Klein, H.; Jacob, E.; Krossing, I. Poly (oxymethylene) dimethyl ether synthesis–a combined chemical equilibrium investigation towards an increasingly efficient and potentially sustainable synthetic route. *Reaction Chemistry & Engineering* **2017**, *2*, 50–59.

(23) Zhang, J.; Shi, M.; Fang, D.; Liu, D. Reaction kinetics of the production of polyoxymethylene dimethyl ethers from methanol and formaldehyde with acid cation exchange resin catalyst. *Reaction Kinetics, Mechanisms and Catalysis* **2014**, *113*, 459–740.

(24) Zhang, J.; Fang, D.; Liu, D. Evaluation of Zr–alumina in production of polyoxymethylene dimethyl ethers from methanol and formaldehyde: performance tests and kinetic investigations. *Industrial & Engineering Chemistry Research* **2014**, *53*, 13589–13597.

(25) Schmitz, N.; Homberg, F.; Berje, J.; Burger, J.; Hasse, H. Chemical equilibrium of the synthesis of poly (oxymethylene) dimethyl ethers from formaldehyde and methanol in aqueous solutions. *Industrial & Engineering Chemistry Research* **2015**, *54*, 6409–6417.

(26) Schmitz, N.; Burger, J.; Hasse, H. Reaction kinetics of the formation of poly (oxymethylene) dimethyl ethers from formaldehyde and methanol in aqueous solutions. *Industrial & Engineering Chemistry Research* **2015**, *54*, 12553–12560.

(27) Oestreich, D.; Lautenschütz, L.; Arnold, U.; Sauer, J. Reaction kinetics and equilibrium parameters for the production of oxymethylene dimethyl ethers (OME) from methanol and formaldehyde. *Chemical Engineering Science* **2017**, *163*, 92–104.

(28) Schmitz, N.; Breitkreuz, C. F.; Ströfer, E.; Burger, J.; Hasse, H. Separation of water from mixtures containing formaldehyde, water, methanol, methylal, and poly (oxymethylene) dimethyl ethers by pervaporation. *Journal of Membrane Science* **2018**, *564*, 806–812.

(29) Li, X. Y.; Yu, H. B.; Sun, Y. M.; Wang, H. B.; Guo, T.; Sui, Y. L.; Miao, J.; Zeng, X. J.; Li, S. P. Synthesis and application of polyoxymethylene dimethyl ethers. Applied Mechanics and Materials. 2014; pp 2969–2973.

(30) Oestreich, D.; Lautenschütz, L.; Arnold, U.; Sauer, J. Production of oxymethylene dimethyl ether (OME)-hydrocarbon fuel blends in a one-step synthesis/extraction procedure. *Fuel* **2018**, *214*, 39–44.

(31) Liu, F.; Wang, T.; Zheng, Y.; Wang, J. Synergistic effect of Brønsted and Lewis acid sites for the synthesis of polyoxymethylene dimethyl ethers over highly efficient SO 4 2-/TiO 2 catalysts. *Journal of Catalysis* **2017**, *355*, 17–25.

(32) Shi, G.-F.; Miao, J.; Wang, G.-Y.; Su, J.-M.; Liu, H.-X. Synthesis of Polyoxymethylene Dimethyl Ethers Catalyzed by Rare Earth Compounds. *Asian Journal of Chemistry* **2015**, *27*.

(33) Zhao, Y.; Xu, Z.; Chen, H.; Fu, Y.; Shen, J. Mechanism of chain propagation for the synthesis of polyoxymethylene dimethyl ethers. *Journal of Energy Chemistry* **2013**, *22*, 833–836.

(34) Zheng, Y.; Tang, Q.; Wang, T.; Liao, Y.; Wang, J. Synthesis of a green fuel additive over cation resins. *Chemical Engineering & Technology* **2013**, *36*, 1951–1956.

(35) Zheng, Y.; Tang, Q.; Wang, T.; Wang, J. Kinetics of synthesis of polyoxymethylene dimethyl ethers from paraformaldehyde and dimethoxymethane catalyzed by ion-exchange resin. *Chemical Engineering Science* **2015**, *134*, 758–766.

(36) Reuss, G.; Disteldorf, W.; Gamer, A. O.; Hilt, A. Formaldehyde. *Ullmann's Encyclopedia of Industrial Chemistry* **2000**,

(37) Burger, J.; Siegert, M.; Ströfer, E.; Hasse, H. Poly (oxymethylene) dimethyl ethers as components of tailored diesel fuel: Properties, synthesis and purification concepts. *Fuel* **2010**, *89*, 3315–3319.

(38) Burger, J. A novel process for the production of diesel fuel additives by hierarchical design. Ph.D. thesis, Techn. Univ. Kaiserslautern, 2012.

(39) Burger, J.; Strofer, E.; Hasse, H. Chemical equilibrium and reaction kinetics of the heterogeneously catalyzed formation of poly (oxymethylene) dimethyl ethers from methylal and trioxane. *Industrial & Engineering Chemistry Research* **2012**, *51*, 12751–12761.

(40) Burger, J.; Hasse, H. Multi-objective optimization using reduced models in conceptual design of a fuel additive production process. *Chemical Engineering Science* **2013**, *99*, 118–126.

(41) Burger, J.; Ströfer, E.; Hasse, H. Production process for diesel fuel components poly (oxymethylene) dimethyl ethers from methane-based products by hierarchical optimization with varying model depth. *Chemical Engineering Research and Design* **2013**, *91*, 2648–2662.

(42) Wang, L.; Wu, W.-T.; Chen, T.; Chen, Q.; He, M.-Y. Ion-Exchange Resin–Catalyzed Synthesis of Polyoxymethylene Dimethyl Ethers: A Practical and Environmentally

Friendly Way to Diesel Additive. *Chemical Engineering Communications* **2014**, *201*, 709–717.

(43) Wu, Q.; Wang, M.; Hao, Y.; Li, H.; Zhao, Y.; Jiao, Q. Synthesis of polyoxymethylene dimethyl ethers catalyzed by Brønsted acid ionic liquids with alkanesulfonic acid groups. *Industrial & Engineering Chemistry Research* **2014**, *53*, 16254–16260.

(44) Wu, J.; Zhu, H.; Wu, Z.; Qin, Z.; Yan, L.; Du, B.; Fan, W.; Wang, J. High Si/Al ratio HZSM-5 zeolite: an efficient catalyst for the synthesis of polyoxymethylene dimethyl ethers from dimethoxymethane and trioxymethylene. *Current Green Chemistry* **2015**, *17*, 2353–2357.

(45) Wu, Y.; Li, Z.; Xia, C. Silica-gel-supported dual acidic ionic liquids as efficient catalysts for the synthesis of polyoxymethylene dimethyl ethers. *Industrial & Engineering Chemistry Research* **2016**, *55*, 1859–1865.

(46) Lautenschütz, L. P. Neue Erkenntnisse in der Syntheseoptimierung oligomerer Oxymethylendimethylether aus Dimethoxymethan und Trioxan. Ph.D. thesis, Ruprecht-Karls-Universitt Heidelberg, 2015.

(47) Lautenschütz, L.; Oestreich, D.; Haltenort, P.; Arnold, U.; Dinjus, E.; Sauer, J. Efficient synthesis of oxymethylene dimethyl ethers (OME) from dimethoxymethane and trioxane over zeolites. *Fuel Processing Technology* **2017**, *165*, 27–33.

(48) Grützner, T.; Hasse, H.; Lang, N.; Siegert, M.; Ströfer, E. Development of a new industrial process for trioxane production. *Chemical Engineering Science* **2007**, *62*, 5613–5620.

(49) Grützner, T. Entwicklung eines destillationsbasierten Verfahrens zur Herstellung von Trioxan. Ph.D. thesis, Techn. Univ. Kaiserslautern, 2007.

(50) Zhang, Q.; Tan, Y.; Liu, G.; Zhang, J.; Han, Y. Rhenium oxide-modified H 3 PW 12 O 40/TiO 2 catalysts for selective oxidation of dimethyl ether to dimethoxy dimethyl ether. *Green Chemistry* **2014**, *16*, 4708–4715.

(51) Zhang, Q.; Wang, W.; Zhang, Z.; Han, Y.; Tan, Y. Low-temperature oxidation of dimethyl ether to polyoxymethylene dimethyl ethers over CNT-supported rhenium catalyst. *Catalysts* **2016**, *6*, 43.

(52) Haltenort, P.; Hackbarth, K.; Oestreich, D.; Lautenschütz, L.; Arnold, U.; Sauer, J. Heterogeneously catalyzed synthesis of oxymethylene dimethyl ethers (OME) from dimethyl ether and trioxane. *Catalysis Communications* **2018**, *109*, 80–84.

(53) Breitkreuz, C. F.; Schmitz, N.; Ströfer, E.; Burger, J.; Hasse, H. Design of a Production Process for Poly (oxymethylene) Dimethyl Ethers from Dimethyl Ether and Trioxane. *Chemie Ingenieur Technik* **2018**, *90*, 1489–1496.

(54) Bongartz, D.; Burre, J.; Mitsos, A. Production of Oxymethylene Dimethyl Ether from Hydrogen and Carbon Dioxide – Part I: Modeling and Analysis for OME_1. *In Press: Industrial & Engineering Chemistry Research* **27 February 2019**,

(55) Ryll, O.; Blagov, S.; Hasse, H. inf/inf-Analysis of homogeneous distillation processes. *Chemical Engineering Science* **2012**, *84*, 315–332.

(56) Grützner, T.; Hasse, H. Solubility of formaldehyde and trioxane in aqueous solutions. *Journal of Chemical & Engineering Data* **2004**, *49*, 642–646.

(57) Chen, J.; Song, H.; Xia, C.; Zhang, X.; Tang, Z. Method for synthesizing polyoxymethylene dimethyl ethers by ionic liquid catalysis. Google Patents, 2010; US Patent App. 12/548,807.

(58) Chen, J.; Song, H.; Xia, C.; Li, Z. Method for synthesizing polyoxymethylene dimethyl ethers catalyzed by an ionic liquid. Google Patents, 2011; US Patent App. 13/154,359.

(59) Xue, Z.; Shang, H.; Xiong, C.; Lu, C.; An, G.; Zhang, Z.; Cui, C.; Xu, M. Synthesis of polyoxymethylene dimethyl ethers catalyzed by sulfonic acid-functionalized mesoporous SBA-15. *RSC Advances* **2017**, *7*, 20300–20308.

(60) Stroefer, E.; Schelling, H.; Hasse, H.; Blagov, S. Method for the production of polyoxymethylene dialkyl ethers from trioxan and dialkylethers. Google Patents, 2011; US Patent 7,999,140.

(61) Arvidson, M.; Fakley, M.; Spencer, M. Lithium halide-assisted formation of polyoxymethylene dimethyl ethers from dimethoxymethane and formaldehyde. *Journal of molecular catalysis* **1987**, *41*, 391–393.

(62) Maurer, G. Vapor-liquid equilibrium of formaldehyde-and water-containing multicomponent mixtures. *AIChE journal* **1986**, *32*, 932–948.

(63) Gruznov, A.; Oreshenkova, E.; Klyuchnikov, V.; Curtis, P. Kinetic studies of the formation of methanol and formic acid in aqueous formaldehyde solutions in the presence of acids. *International polymer science and technology* **1997**, *24*, 39–43.

(64) Balashov, A.; Krasnov, V.; Danov, S.; Chernov, A. Y.; Sulimov, A. Formation of cyclic oligomers in concentrated aqueous solutions of formaldehyde. *Journal of Structural Chemistry* **2001**, *42*, 398–403.

(65) Bernard, K. A.; Atwood, J. D. Evidence for carbon-oxygen bond formation, aldehyde decarbonylation, and dimerization by reaction of formaldehyde and acetaldehyde with trans-ROIr (CO)(PPh3) 2. *Organometallics* **1988**, *7*, 235–236.

(66) Albert, M.; García, B. C.; Kreiter, C.; Maurer, G. Vapor-liquid and chemical equilibria of formaldehyde-water mixtures. *AIChE Journal* **1999**, *45*, 2024–2033.

(67) Albert, M. Thermodynamische Eigenschaften formaldehydhaltiger Mischungen. Ph.D. thesis, Techn. Univ. Kaiserslautern, 1998.

(68) Hahnenstein, I.; Hasse, H.; Kreiter, C. G.; Maurer, G. 1H-and 13C-NMR-spectroscopic study of chemical equilibria in solutions of formaldehyde in water, deuterium oxide, and methanol. *Industrial & engineering chemistry research* **1994**, *33*, 1022–1029.

(69) Hahnenstein, I.; Albert, M.; Hasse, H.; Kreiter, C. G.; Maurer, G. NMR spectroscopic and densimetric study of reaction kinetics of formaldehyde polymer formation in water, deuterium oxide, and methanol. *Industrial & engineering chemistry research* **1995**, *34*, 440–450.

(70) Kuhnert, C.; Albert, M.; Breyer, S.; Hahnenstein, I.; Hasse, H.; Maurer, G. Phase equilibrium in formaldehyde containing multicomponent mixtures: experimental results for fluid phase equilibria of (formaldehyde+(water or methanol)+ methylal)) and (formaldehyde+ water+ methanol+ methylal) and comparison with predictions. *Industrial & engineering chemistry research* **2006**, *45*, 5155–5164.

(71) Ott, M. Reaktionskinetik und Destillation formaldehydhaltiger Mischungen. Ph.D. thesis, Techn. Univ. Kaiserslautern, 2004.

(72) Fredenslund, A.; Jones, R. L.; Prausnitz, J. M. Group-contribution estimation of activity coefficients in nonideal liquid mixtures. *AIChE Journal* **1975**, *21*, 1086–1099.

(73) Renon, H.; Prausnitz, J. M. Local compositions in thermodynamic excess functions for liquid mixtures. *AIChE journal* **1968**, *14*, 135–144.

(74) Mitsos, A.; Bollas, G. M.; Barton, P. I. Bilevel Optimization Algorithm for Rigorous & Robust Parameter Estimation in Thermodynamics BOARPET. `http://www.avt.rwth-aachen.de/cms/AVT/Wirtschaft/SoftwareSimulation/~kvkz/BOARPET/?lidx=1`, Accessed: 2018-03-22.

(75) Mitsos, A.; Bollas, G. M.; Barton, P. I. Bilevel optimization formulation for parameter estimation in liquid–liquid phase equilibrium problems. *Chemical Engineering Science* **2009**, *64*, 548–559.

(76) Bollas, G. M.; Barton, P. I.; Mitsos, A. Bilevel optimization formulation for parameter estimation in vapor–liquid (–liquid) phase equilibrium problems. *Chemical Engineering Science* **2009**, *64*, 1768–1783.

(77) König, D. H.; Baucks, N.; Dietrich, R.-U.; Wörner, A. Simulation and evaluation of a process concept for the generation of synthetic fuel from CO_2 and H_2. *Energy* **2015**, *91*, 833–841.

(78) Van-Dal, É. S.; Bouallou, C. Design and simulation of a methanol production plant from CO_2 hydrogenation. *Journal of Cleaner Production* **2013**, *57*, 38–45.

(79) Ursua, A.; Gandia, L. M.; Sanchis, P. Hydrogen production from water electrolysis: current status and future trends. *Proceedings of the IEEE* **2012**, *100*, 410–426.

(80) Smolinka, T.; Günther, M.; Garche, J. Stand und Entwicklungspotenzial der Wasserelektrolyse zur Herstellung von Wasserstoff aus regenerativen Energien. *Kurzfassung des Abschlussberichtes NOW-Studie, Freiburg im Breisgau* **2011**,

(81) Lee, U.; Burre, J.; Caspari, A.; Kleinekorte, J.; Schweidtmann, A. M.; Mitsos, A. Techno-economic optimization of a green-field post-combustion CO_2 capture process using superstructure and rate-based models. *Industrial & Engineering Chemistry Research* **2016**, *55*, 12014–12026.

(82) Wagemann, K.; Ausfelder, F. E-Fuels – Mehr als eine Option. *DECHEMA* **2017**,

Abstract Graphic